MATERIALE PLASTICE
https://revmaterialeplastice.ro
https://doi.org/10.37358/Mat.Plast.1964

Effect of Corrected Extrusion Flow Rate on Wall Thickness Error of MEAM Thin-walled Model

CHEN WANG[1,2]*, JINGYAO LI[1,2], CHENYUN ZHANG[1,2]
[1] Nanjing Forestry University, College of Furnishings and Industrial Design, 159 Longpan Road, Nanjing Jiangsu, China
[2] Jiangsu Co-Innovation Center of Efficient Processing and Utilization of Forest Resources, 159 Longpan Road, Jiangsu, China

Abstract: *In order to solve the wall thickness error problem of filament-based extrusion additive manufacturing (MEAM) of thin-walled model and to improve the printing accuracy of MEAM thin-walled model. In this study, a square thin-walled model A was designed as the experimental specimen, and a wall thickness error correction method based on pre-experiment was proposed, by which the corrected extrusion flow rate R was calculated to be 92.8%. Model A was reprinted using the corrected extrusion flow rate (92.8%), and the wall thickness error of model A printed using the corrected extrusion flow rate was found to be significantly reduced by spiral micrometer measurement. When model A was observed through an industrial microscope, it can be seen from the sidewall surface detail diagram that the surface of model A printed with the corrected extrusion flow rate has no bumps, cracks and other structures, and the surface quality is better; moreover, it can be seen from the cross-sectional dimension diagram that the wall thickness (0.403 mm) of model A printed with the corrected extrusion flow rate (92.8%) is significantly reduced compared to the wall thickness (0.472 mm) of model A printed with the default extrusion flow rate (100%), and is close to the designed wall thickness (0.400 mm), which further verifies that the wall thickness error of the MEAM thin-walled model with the corrected extrusion flow rate has been significantly reduced.*

Keywords*: Corrected extrusion flow rate, MEAM, Thin-walled model, Wall thickness error*

1. Introduction

Filament based material extrusion additive manufacturing (MEAM) is one of the most commonly used technologies in 3D printing. MEAM technology constructs product prototypes layer by layer by extruding molten filament through the nozzle, which has the characteristics of simple moulding principle, convenient operation and wide application range [1-3]. Extrusion flow rate, one of the main process parameters of MEAM technology, refers to the amount of molten filament extruded from the nozzle per second. In 3D printing slicing software, extrusion flow rate is commonly expressed as extrusion rate, which is the ratio of actual extrusion flow rate to standard extrusion flow rate [4]. Among them, the standard extrusion flow rate is a fixed value set at the factory based on the performance parameters of the 3D printer (printing speed, nozzle diameter, etc.) [5]. Currently, the standard extrusion flow rate of most 3D printers on the market is within the range of 1~30 mm^3/s [6].

Normally, the default extrusion rate in the slicing software is 100%, i.e. the actual extrusion flow rate is equal to the standard extrusion flow rate [7]. However, during the actual slicing process, the extrusion rate needs to be reset according to the filament characteristics and model printing requirements [8]. For example, when the extrusion rate is set to 105%, this means that the actual extrusion flow rate is 5% more than the standard extrusion flow rate, i.e., 5% more molten filament is extruded from the nozzle per second. Extrusion flow rate settings are many times not successful at once, and several trials are needed to get the desired parameters [9]. The quality of the 3D printed model can be affected by setting the extrusion flow rate too high or too low [10]. When the extrusion flow rate is too high, too much molten filament is extruded from the nozzle, which will easily lead to problems such as overflow and bumps in the model; when the extrusion flow rate is too low, not enough molten filament is extruded from the nozzle, which will easily lead to problems such as holes and cracks in the model [11-13].

**email: 996869559@qq.com*

A thin-walled model is a model whose ratio of thickness to other feature dimensions (e.g., length or width of the model) is less than 0.1 [14]. Thin-walled models exist in large numbers in MEAM technology, especially the shells of various product prototypes (e.g., the shells of electronic products and daily necessities) are mostly in the form of thin walls [15, 16]. However, when 3D printing of thin-walled model is performed, the problem of inconsistency between the actual wall thickness and the designed wall thickness often occurs, which is caused by the moulding principle of MEAM technology [17]. In order to solve the wall thickness error problem of MEAM thin-walled model, this study reduces the wall thickness error and improves the printing accuracy of MEAM thin-walled model by correcting the extrusion flow rate.

2. Materials and methods

2.1. Materials

The PLA filament (1.75 mm diameter, White, Anycubic, Shenzhen, China) was used for 3D printing by MEAM technology.

2.2. Specimen preparation

In order to measure the wall thickness error of the MEAM thin-walled model, the SolidWorks software was used to design the square model A (3D size 40*40*40 mm), which is a hollow structure with the designed thicknesses of the four side walls of 0.400 mm, as shown in Figure 1. The thin-walled model A was imported into Cura software for slicing, and the extrusion flow rate was set to the default value of 100%, the extrusion width was 0.4 mm, and the layer height was 0.2 mm. The sliced file was imported into a MEAM 3D printer (0.4 mm nozzle diameter, Anycubic, Shenzhen, China) for specimen fabrication.

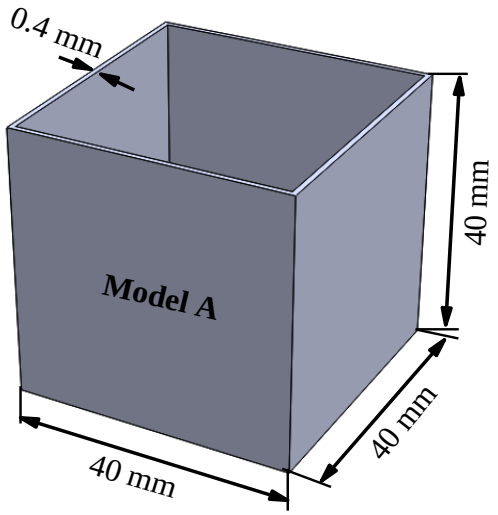

Figure 1. The square model A

2.3. Performance test

A spiral micrometer (Range 0~25 mm, Accuracy 0.001 mm, Miracle, Suzhou, China) was used to measure the wall thickness dimensions of the MEAM thin-walled model, and the centre points of the four sides of the thin-walled model were selected as the measurement points, and the measurement schematic is shown in Figure 2.

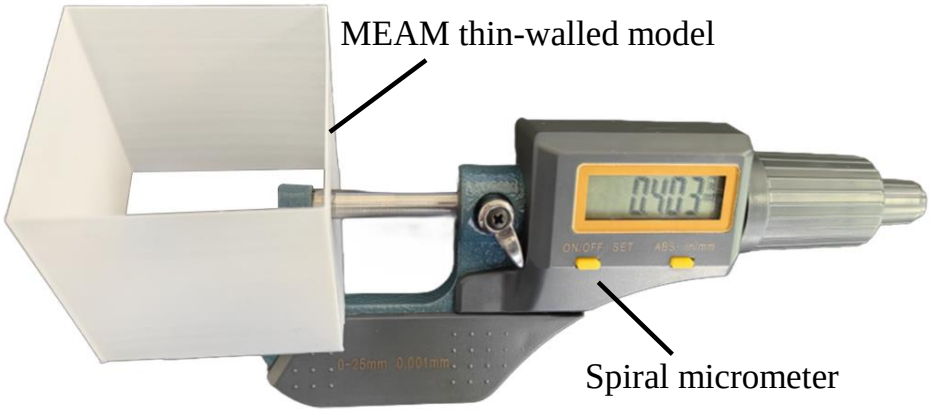

Figure 2. Measurement schematic

An industrial microscope (CL-MA-50M, Colomer, Guangzhou, China) was used to observe the details of the MEAM thin-walled model.

3. Results and discussions

3.1. Principle of wall thickness error formation in MEAM thin-walled model

As shown in Figure 3, the wall thickness error of the MEAM thin-walled model is formed as follows: since the PLA molten filament just extruded from the nozzle is in the viscous flow state, the PLA molten filament produces bulging deformation in the horizontal direction under the action of gravity and extrusion pressure, which increases the width of the PLA molten filament, and makes the cross-sectional shape of the solidified PLA filament approximate to an oval shape [18-20]. This causes the actual thickness of the MEAM thin-walled model to be larger than the designed thickness, and the wall thickness error arises as a result.

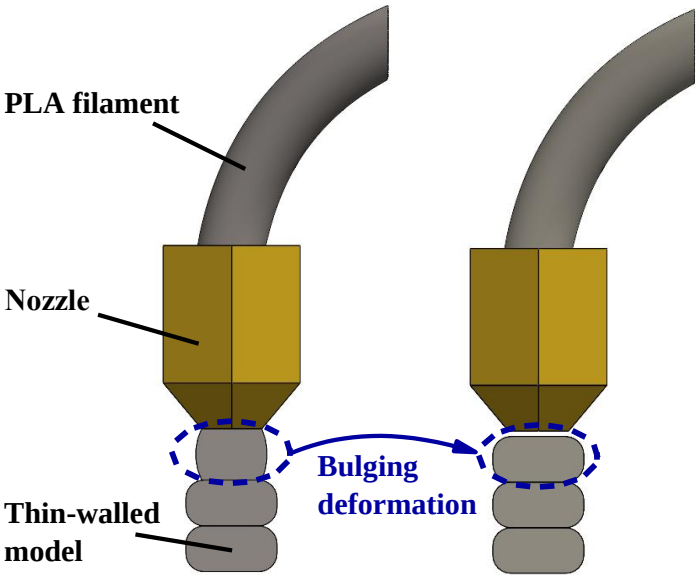

Figure 3. Principle diagram

3.2. Method for correcting wall thickness error in MEAM thin-walled model

Due to the different structures and wall thicknesses of different MEAM thin-walled models, their wall thickness errors cannot be calculated and predicted by a uniform formula [21]. Therefore, this study proposes a wall thickness error correction method based on pre-experiment, i.e., the model is first printed by pre-experiment using the default extrusion flow rate (100%). Then, by measuring the thickness of each thin wall (W_1, W_2, ⋯, W_n) in the pre-experimental model, the average thickness of each thin wall is

calculated, and the difference between the average thickness and the designed wall thickness W_0 is calculated to obtain the wall thickness error ΔW, the calculation formula is as follows: $\Delta W = \frac{W_1+W_2+\cdots+W_n}{n} - W_0$. Finally, based on the wall thickness error ΔW, the corrected extrusion flow rate R is calculated using the following formula: $R = (1 - \Delta W) \times 100\%$.

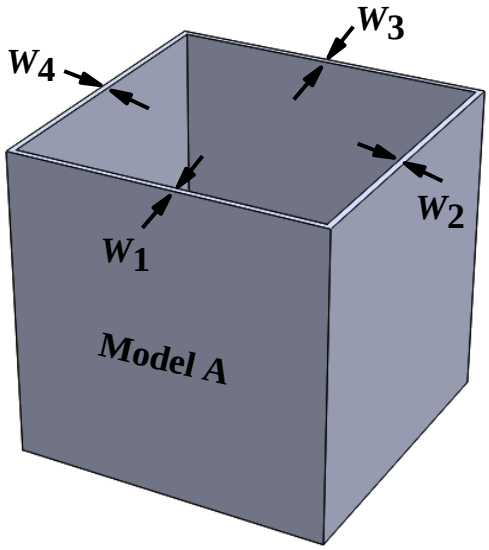

Figure 4. Pre-experimental model A

Taking model A as an example, the pre-experimental model was first printed with 100% extrusion flow rate, and the thicknesses of the four thin walls of the pre-experimental model, W_1, W_2, W_3, and W_4 (Figure 4), were measured with the values of 0.469, 0.471, 0.472, and 0.476 mm, respectively. Then, the average of the four thicknesses (0.472 mm) was taken and the difference was calculated with the designed wall thickness W_0 (0.400 mm) to obtain the wall thickness error ΔW (0.072 mm) for model A. Finally, based on the wall thickness error ΔW, the corrected extrusion flow rate R was calculated to be 92.8%.

3.3. Effect of corrected extrusion flow rate on wall thickness error of MEAM model

Model A was reprinted using the corrected extrusion flow rate (92.8%), and the thicknesses W_1, W_2, W_3, and W_4 of the four thin walls of model A were measured by a spiral micrometer, and the results of the measurements were 0.402, 0.404, 0.405, and 0.401 mm, respectively (Figure 5). Compared with the designed wall thickness W_0, the errors of W_1, W_2, W_3, and W_4 are all smaller, indicating that the wall thickness error of model A printed using the corrected extrusion flow rate is significantly reduced. This is because as the extrusion flow rate decreases, the amount of PLA molten filament extruded from the nozzle per second decreases, and the extrusion pressure action of the nozzle decreases, resulting in a decrease in the area of PLA molten filament spreading in the horizontal direction, that is, the actual extrusion width decreases [22-24]. As a result, the wall thickness error of the MEAM thin-walled model is significantly reduced after the extrusion flow rate correction.

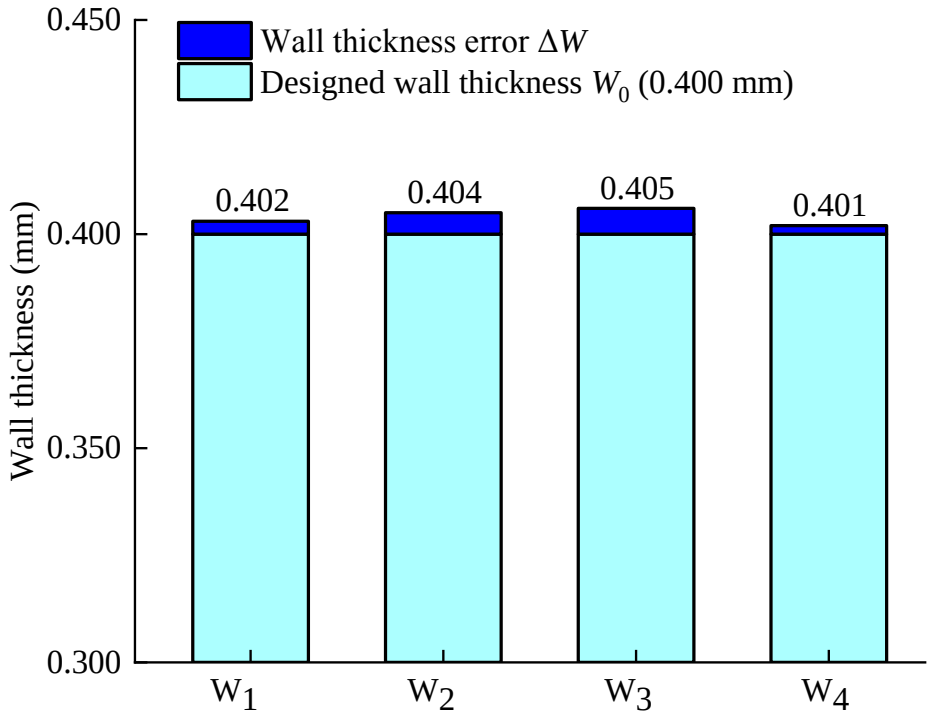

Figure 5. Effect of corrected extrusion flow rate on wall thickness error of MEAM model

3.4. Comparison of details of MEAM thin-walled model

In order to visually compare the correction effect of extrusion flow rate, an industrial microscope was used to observe and measure model A printed with the corrected extrusion flow rate (92.8%) and the default extrusion flow rate (100%), including observing the details of the sidewall surface and measuring the cross-sectional dimensions. Two sets of models were photographed using the industrial microscope, and the detailed sidewall surface and cross-sectional dimension images obtained are shown in Figures 6 and 7. Figure 7 used the measurement software of the industrial microscope to measure the wall thickness of the model.

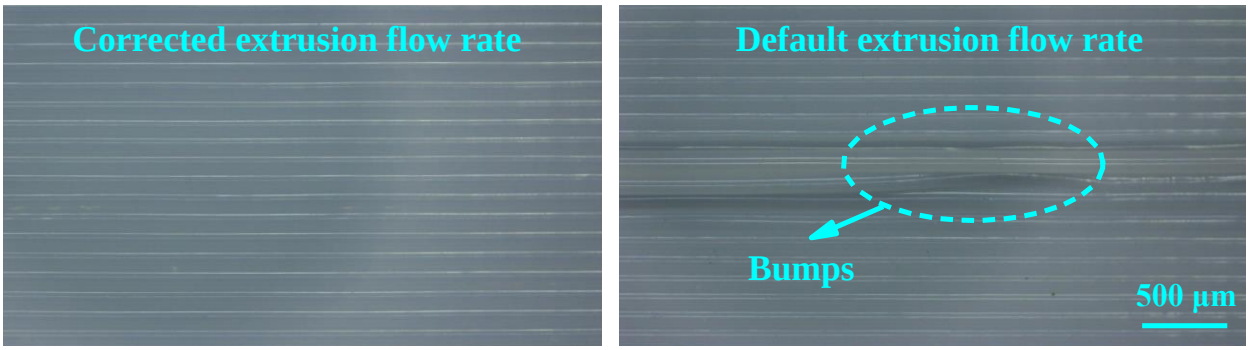

Figure 6. Sidewall surface detail diagram

From the sidewall surface detail diagram (Figure 6), it can be seen that the surface of model A printed with the corrected extrusion flow rate has no bumps, cracks and other structures, and the surface quality is better. In contrast, the model A printed with the default extrusion flow rate has bump structures on the surface, indicating that the printing filament is over-extruded, which affects the surface quality of the model [25].

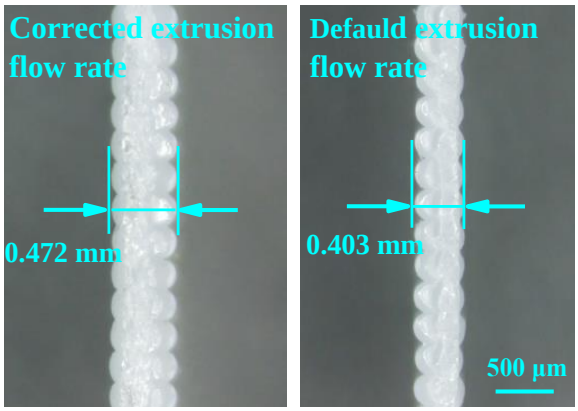

Figure 7. Cross-sectional dimension diagram

From the cross-sectional dimension diagram (Figure 7), it can be seen that compared with the wall thickness (0.472 mm) of model A printed with the default extrusion flow rate , the wall thickness (0.403 mm) of model A printed with the corrected extrusion flow rate is significantly reduced and is close to the designed wall thickness (0.400 mm), which further verifies that the wall thickness error of the MEAM thin-walled model with the corrected extrusion flow rate is significantly reduced.

4. Conclusions

In this study, a square thin-walled model A was designed as the experimental specimen, and a wall thickness error correction method based on pre-experiment was proposed, by which the corrected extrusion flow rate R was calculated to be 92.8%. The corrected extrusion flow rate was used to reprint model A. It was measured and found the wall thickness error of the MEAM thin-walled model with the corrected extrusion flow rate was significantly reduced.

Observing model A through an industrial microscope, as seen in the sidewall surface detail diagram, the surface of model A printed with the corrected extrusion flow rate has no bumps, cracks and other structures, and the surface quality is better. From the cross-sectional dimension diagram, it can be seen that compared with the model A printed with the default extrusion flow rate, the wall thickness error of the model A printed with the modified corrected flow rate is significantly reduced.

References

1.YILMAZ, M., YILMAZ, N. F., KALKAN, M. F., Rheology, crystallinity, and mechanical investigation of interlayer adhesion strength by thermal annealing of polyetherimide (PEI/ULTEM 1010) parts produced by 3D printing. *Journal of Materials Engineering and Performance*, 2022, 31(12), 9900-9909. DOI: 10.1007/s11665-022-07049-z

2. WANG, Y. Q., LIU, Z. G., GU, H. W., CUI, C. Z., HAO, J. B., Improved mechanical properties of 3D-printed SiC/PLA composite parts by microwave heating. *Journal of Materials Research*, 2019, 34(20), 3412-3419. DOI: 10.1557/jmr.2019.296

3. YANG, Z. Z., FENG, X. H., XU, M., RODRIGUE, D., Printability and properties of 3D printed poplar fiber/polylactic acid biocomposites. *BioResources*, 2022, 16(2), 2774-2788.
DOI: 10.15376/biores.16.2.2774-2788

4.YANG, L., LIU, D., GUO, R., JI, Z. Y., WANG, X. L., SHI, X. Y., Flexibility of Diels-Alder reversible covalent bonds in fused deposition modeling 3D printing: Bonding and de-bonding. *Polymer*, 2023, 266:125637. DOI: 10.1016/j.polymer.2022.125637

5.ZOU, Y. M., XIA, Y. X., YAN, X. X., Effect of melamine formaldehyde resin encapsulated UV acrylic resin primer microcapsules on the properties of UV primer coating. *Polymers*, 2024, 16(16), 2308.
DOI: 10.3390/polym16162308

6.WANG, L., HAN, Y., YAN, X. X., Effects of adding methods of fluorane microcapsules and shellac resin microcapsules on the preparation and properties of bifunctional waterborne coatings for basswood. *Polymers*, 2022, 14(18), 3919. DOI: 10.3390/polym14183919
7. ZHANG, R., YU, L. G., CHEN, K., XUE, P., JIA, M. Y., HUA, Z. T., Amelioration of interfacial properties for CGF/PA6 composites fabricated by ultrasound-assisted FDM 3D printing. *Composites Communications*, 2023, 39(20):101551. DOI: 10.1016/j.coco.2023.101551
8. WANG, Q., FENG, X. H., LIU, X. Y., Functionalization of nanocellulose using atom transfer radical polymerization and applications: A review. *Cellulose*, 2023, 30, 8495-8537.
DOI: 10.1007/s10570-023-05403-5
9. DING, T. T., YAN, X. X., ZHAO, W. T., Effect of urea–formaldehyde resin–coated colour-change powder microcapsules on performance of waterborne coatings for wood surfaces. *Coatings*, 2022, 12(9), 1289. DOI: 10.3390/coatings12091289
10. HAN, Y., YAN, X. X., ZHAO, W. T., Effect of thermochromic and photochromic microcapsules on the surface coating properties for metal substrates. *Coatings*, 2022, 12(11), 1642.9.
DOI: 10.3390/coatings12111642
11. LUO, M., TIAN, X. Y., SHANG, J. F., ZHU, W. J., LI, D. C., QIN, Y. J., Impregnation and interlayer bonding behaviours of 3D-printed continuous carbon-fiber-reinforced poly-ether-ether-ketone composites. *Composites Part A-Applied Science and Manufacturing*, 2019, 121, 130-138.
DOI: 10.1016/j.compositesa.2019.03.020
12. YU, S. L., ZHENG, Q., CHEN, T. Y., ZHANG, H. L., CHEN, X. R., Consumer personality traits vs. their preferences for the characteristics of wood furniture products. *BioResources*, 2023, 18(4), 7443-7459. DOI: 10.15376/biores.18.4.7443-7459
13. ZOU, Y. M., PAN, P., YAN, X. X., Comparative analysis of performance of water-based coatings prepared by two kinds of anti-bacterial microcapsules and nano-silver solution on the surface of andoung wood. *Coatings*, 2023, 13(09), 1518. DOI: 10.3390/coatings13091518
14. MO, X. F., ZHANG, X. H., FANG, L., ZHANG, Y., Research progress of wood-based panels made of thermoplastics as wood adhesives. *Polymers*, 2022, 14(1), 98. DOI: 10.3390/polym14010098
15. LI, W. B., YAN, X. X., ZHAO, W. T., Preparation of crystal violet lactone complex and its effect on discoloration of metal surface coating. *Polymers*, 2022, 14(20), 4443. DOI: 10.3390/polym14204443
16. ZHOU, C. M., HUANG, T., LIANG, S., Smart home R&D system based on virtual reality. *Journal of Intelligent & Fuzzy Systems*, 2020, 40(2), 3045-3054. DOI: 10.3233/JIFS-189343
17. YU, S. L., WU, Z. H., Research on the influence mechanism of short video communication effect of furniture brand: based on ELM model and regression analysis. *BioResources*, 2024, 19(2), 3191-3207.
DOI: 10.15376/biores.19.2.3191-3207
18. LI, R. R., CHEN, J. J., WANG, X.-D., Prediction of the color variation of moso bamboo during CO2 laser thermal modification. *BioResources*, 2020, 15(3), 5049-5057.
DOI: 10.15376/biores.15.3.5049-5057
19. QI, Y. Q., SUN, Y., ZHOU, Z. W., HUANG, Y., LI, J. X, LIU, G. Y., Response surface optimization based on freeze-thaw cycle pretreatment of poplar wood dyeing effect. *Wood Research*, 2023, 68(2), 293-305. DOI: 10.37763/wr.1336-4561/68.2.293305
20. LIU, Q., GU, Y., XU, W., LU, T., LI, W., FAN, H., Compressive properties of green velvet material used in mattress bedding. *Applied Sciences*, 2021, 11(23), 11159. DOI: 10.3390/app112311159
21. FENG, X. H., YANG, Z. Z., WANG, S. Q., WU, Z. H., The reinforcing effect of lignin-containing cellulose nanofibrils in the methacrylate composites produced by stereolithography. *Polymer Engineering and Science*, 2022(9), 2968-2976. DOI: 10.1002/pen.26077
22. YANG, L., HAN, T. Q., LIU, Y. X., Yin, Q., Effects of vacuum heat treatment and wax impregnation on the color of pterocarpus macrocarpus kurz. *BioResources*, 2021, 16(1), 954-963.
DOI: 10.15376/biores.16.1.954-963
23. LIU, Y., HU, J., WU, Z. H., Fabrication of coatings with structural color on a wood surface. *Coatings*, 2020, 10(1), 32. DOI: 10.3390/coatings10010032

24. ZHOU, J. C., XU, W., Toward interface optimization of transparent wood with wood color and texture by silane coupling agent. *Journal of Materials Science*, 2022, 57(10), 5825-5838. DOI: 10.1007/s10853-022-06974-7
25. ZHOU, C. M., HUANG, T., LUO, X., KANER, J., Reorganisation and construction of an age-friendly smart recreational home system: based on function-capability match methodology. *Applied Sciences-Basel*, 2023, 13(7), 9783. DOI: 10.3390/app13179783

Manuscript received: 22.10.2024